Supplementary Information

Highly efficient supported catalysts based on Zr-containing polyoxometalates and multiwalled carbon nanotubes for selective oxidation of thioethers with H_2O_2

Vladimir A. Lopatkin,[a] Vasilii Yu. Evtushok,[a*] Olga A. Stonkus,[a] Lidiya S. Kibis,[a]
Olga Yu. Podyacheva,[a] and Oxana A. Kholdeeva,[a*]
Boreskov Institute of Catalysis, Pr. Lavrentieva 5, Novosibirsk 630090, Russia

Table of Contents

POM Synthesis and Characterization

The synthesis of **$(Bu_4N)_6[\{W_5O_{18}Zr(\mu\text{-}OH)\}_2]$** (**$ZrW_5$**) was carried out as described previously [S1]. Anal. Calcd. (%) for $C_{96}H_{218}N_6Zr_2W_{10}O_{38}$: C, 28.20; H, 5.33; N, 2.06; Zr 4.47; W, 44.99. Found: C, 27.70; H, 5.57; N, 2.02; Zr, 4.58; W, 43.7. IR (KBr, 1000−400 cm^{-1}): 970 (sh, W=O), 945 (s, W=O), 881 (m), 812 (br, WOW), 731 (s, ZrOH), 645 (m), 625 (m), 557 (m), 430 (s), 419 (sh). ^{183}W NMR (ppm, in CD_3CN): 50.8 ($4W_{eq}$), 78.2 ($1W_{ax}$).

The synthesis of **$(Bu_4N)_8[\{PW_{11}O_{39}Zr(\mu\text{-}OH)\}_2]$** (**$PW_{11}Zr$**) was adapted from ref. [S2] as described in [S3]. Anal. Calcd. (%) for $C_{128}H_{294}N_8P_2Zr_2W_{22}O_{82}$: C, 20.37; H, 3.90; N, 1.48; Zr, 2.42; W, 53.59. Found: C, 20.20; H, 3.85; N, 1.5; Zr, 2.33; W, 53.3. IR (1100–400 cm^{-1}): 1064, 965, 890, 807, 768 (ZrOZr), 685, 595, 514. ^{183}W NMR (ppm, 0.02 M in CD_3CN): δ –91.6 (2), –92.6 (2), –96.3 (1), –102.5 (2), –115.5 (2), –119.1 (2). ^{31}P NMR (ppm, 0.01 M in CH_3CN): δ –12.22. Potentiometric titration with Bu_4NOH (0.77 M in CH_3OH) revealed one acid proton per POM molecule, which is in agreement with the literature [S4].

The synthesis of **$(Bu_4N)_{11}H_3[\{P_2W_{17}O_{61}Zr\}_2(\mu\text{-}OH)_2]$** (**$P_2W_{17}Zr$**) was adapted from the literature [S5]. The lacunary precursor $K_{10}[\alpha_2\text{-}P_2W_{17}O_{61}]$ was prepared following the literature protocol [S6]. $ZrOCl_2{\cdot}8H_2O$ (135.5 mg, 0.419 mmol) was dissolved in 24.1 mL of water. Then $K_{10}[\alpha_2\text{-}P_2W_{17}O_{61}]$ (2.0 g, 0.4 mmol) of was added, and the mixture was stirred for 15 min. Next, the pH of the solution was adjusted to 2.5 using 1 M HCl, and the reaction mixture was stirred for 30 min at 90 °C. After cooling to room temperature, 1880 mg of Bu_4NBr (5.838 mmol) was added, and the resulting white solid was separated by filtration, washed two times with water and then with ice ethanol, dried overnight at room temperature, and then dried at 60 °C under dynamic vacuum. The yield of thus obtained Bu_4N-salt of $P_2W_{17}Zr$ was 1.8 g. Anal. Calcd. for $C_{176}H_{401}N_{11}Zr_2P_4W_{34}O_{126}$: C, 18.8; H, 3.6; N, 1.4; Found: C, 18.7; H, 3.4; N, 1.4. IR (1200–400, cm^{-1}): 1149, 1089, 1017, 955, 910, 790, 598, 562, 526, 467. ^{31}P NMR (ppm, 0.02 M in CH_3CN at 20 °C): δ –10.70, –13.27.

The synthesis of **$(Bu_4N)_7[(PW_{11}TiO_{39})_2OH]$** (**$PW_{11}Ti$**) was carried out following the literature protocol [S7]. The number of Bu_4N cations determined by the ignition at 600 °C was ca. 3.5 per P atom. Anal. Calcd. for $C_{112}H_{253}N_7O_{79}P_2Ti_2W_{22}$: C, 18.78; H, 3.56; N, 1.37; O, 17.64; P, 0.86; Ti, 1.34; W, 56.45. Found: C, 19.11; H, 3.58; N, 1.37; P, 0.66; Ti, 1.16; W, 56.33. IR (1200–400, cm^{-1}): δ 1076, 971, 891, 815, 655, 594, 515. ^{31}P NMR (ppm, in dry CH_3CN at 20 °C): δ -12.76. ^{183}W NMR, (ppm, in CH_3CN at 20 °C): δ –89.5 (2), –98.5 (2), –99.2 (1), –101.5 (2), –105.4 (2), –108.7 (2).

The synthesis of **$(Bu_4N)_3[W_5O_{18}Ti(OCH_3)]$** (**Ti-L**) was carried out following the literature protocol [S8]. IR (1200–400, cm^{-1}): δ 1150, 1105, 1055, 1025, 1007, 969, 950, 886, 802, 738, 619, 598, 577, 540, 445. ^{183}W NMR, (ppm, in CD_3CN at 20 °C): δ –42.6 ($4W_{eq}$), –74.5 ($1W_{ax}$).

Additional characterization data, kinetic curves and comparison tables

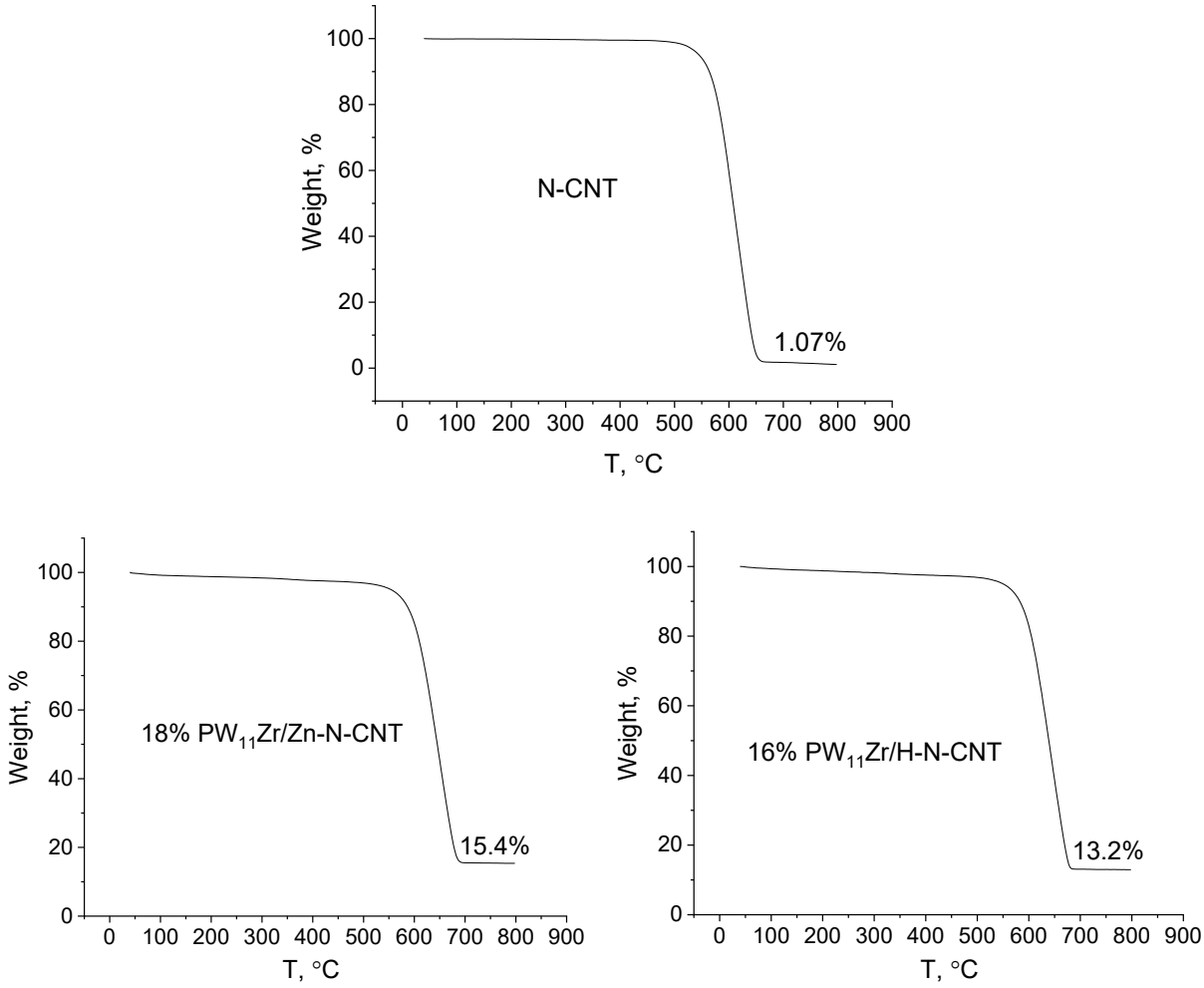

Figure S1. TGA curves for N-CNT support (upper panel) and representative supported $PW_{11}Zr$ catalysts (lower panel).

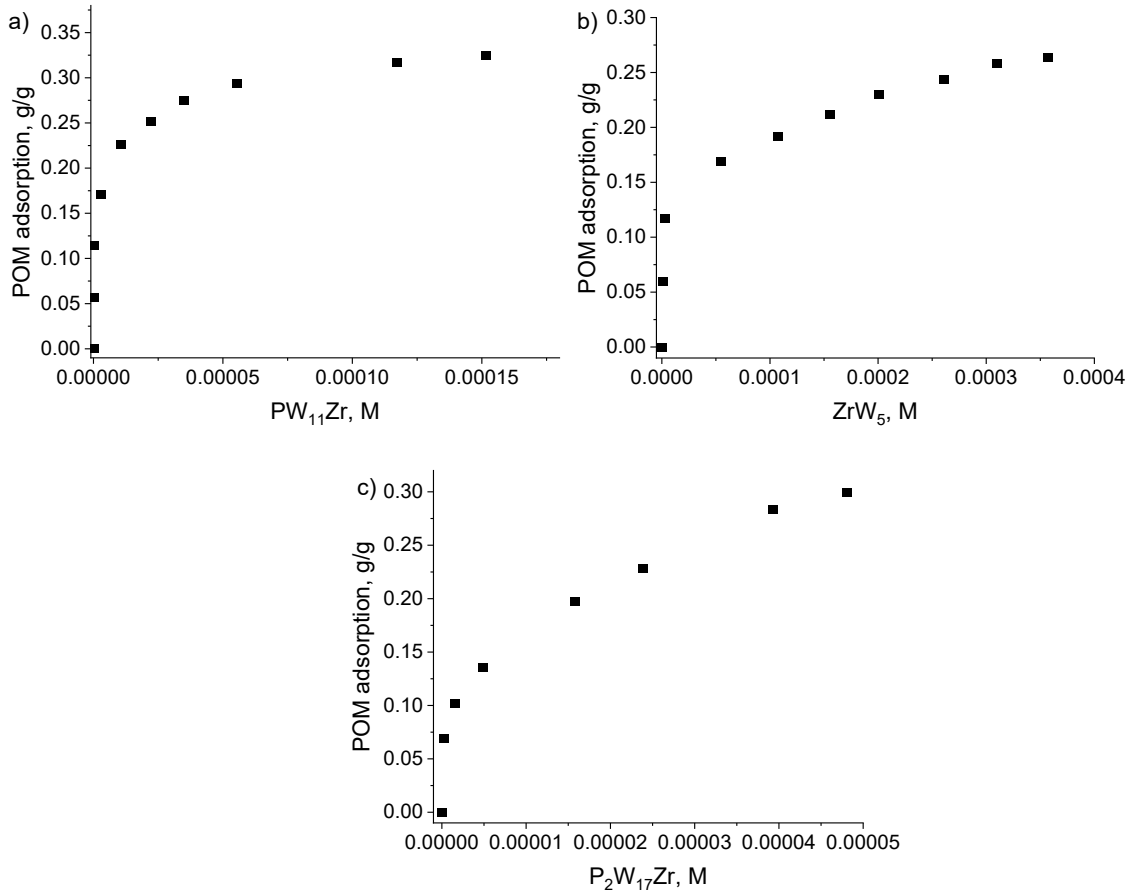

Figure S2. Adsorption isotherms for a) $PW_{11}Zr$, b) ZrW_5 and c) $P_2W_{17}Zr$ adsorption on N-CNT using H^+ as immobilizing agent.

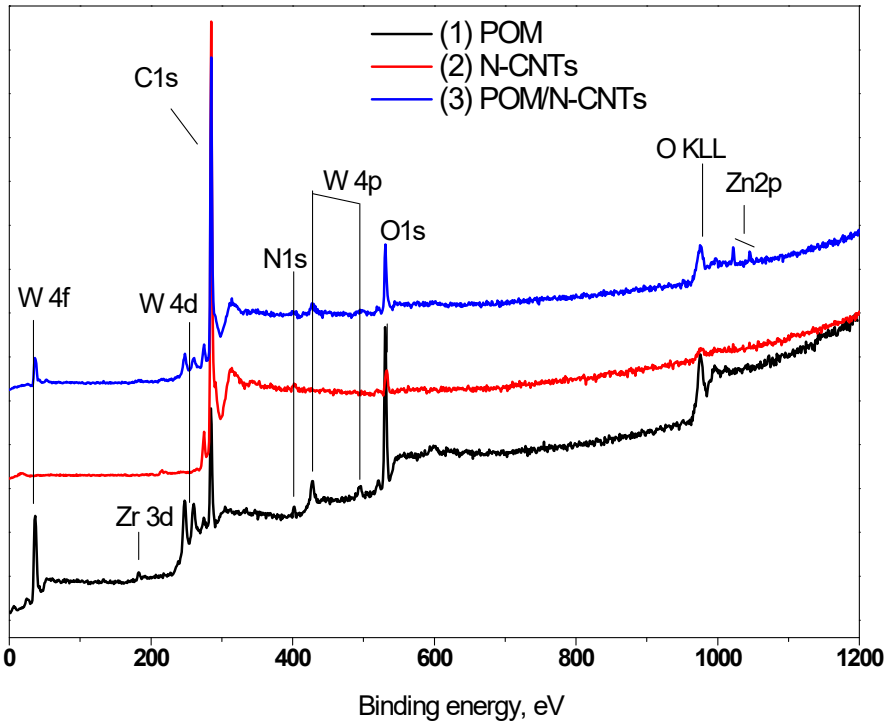

Figure S3. XPS survey spectra of: (1) TBA-salt $PW_{11}Zr$, (2) N-CNT, and (3) $PW_{11}Zr$/Zn-N-CNT.

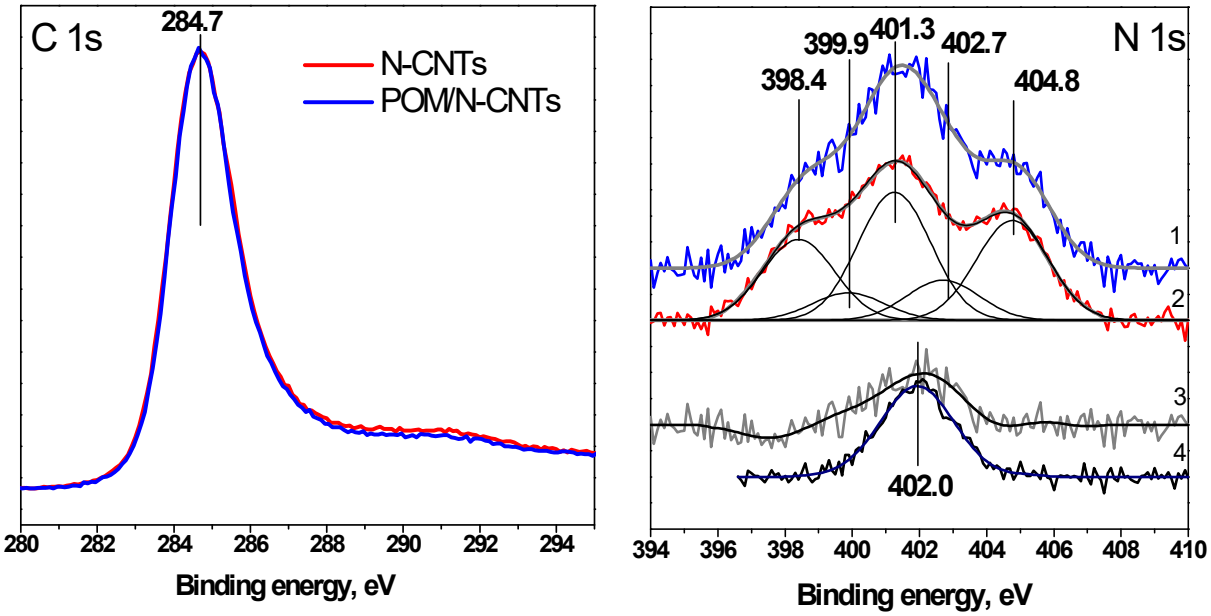

Figure S4. a) C 1s XPS spectra of N-CNT and $PW_{11}Zr$/Zn-N-CNT. b) N 1s XPS spectra of (1) $PW_{11}Zr$/Zn-N-CNT, (2) N-CNT, (3) difference spectrum obtained by subtracting the spectra of samples (1) and (2), and (4) TBA-salt $PW_{11}Zr$.

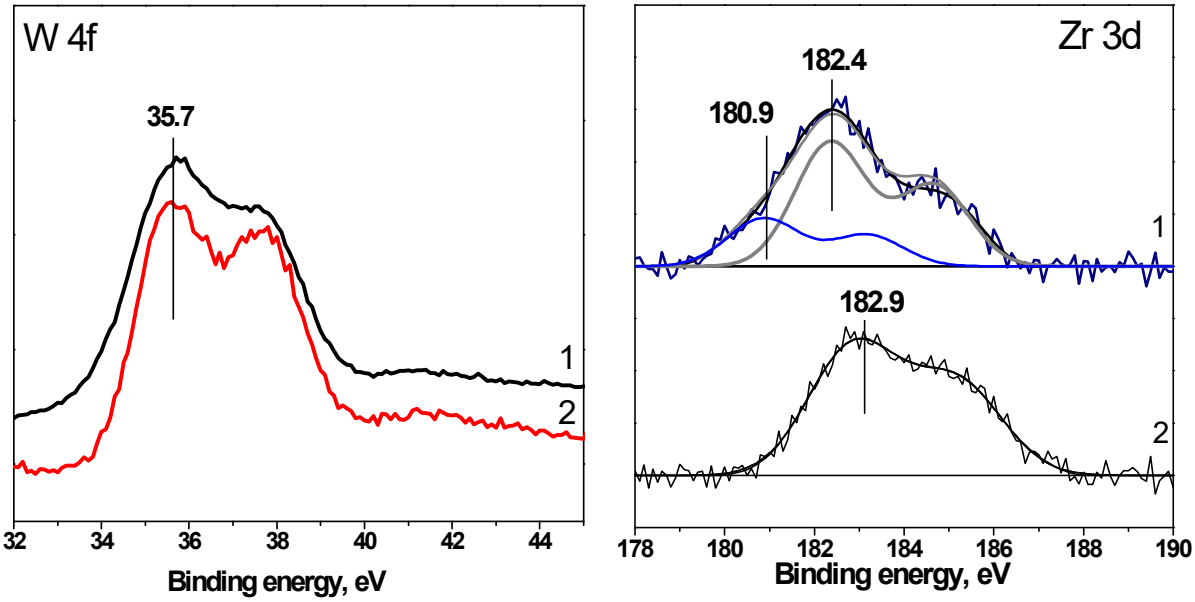

Figure S5. W 4f and Zr 3d XPS spectra of (1) TBA-salt $PW_{11}Zr$ and (2) $PW_{11}Zr$/Zn-N-CNT.

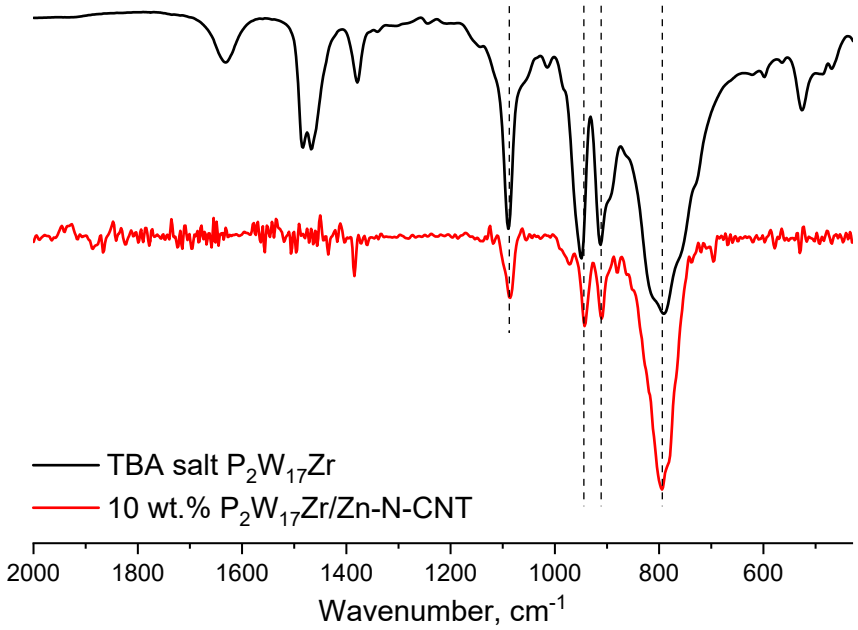

Figure S6. FT-IR spectra of TBA-salt of $P_2W_{17}Zr$ Zr-POMs and corresponding heterogenous catalyst 10% $P_2W_{17}Zr$/Zn-N-CNT.

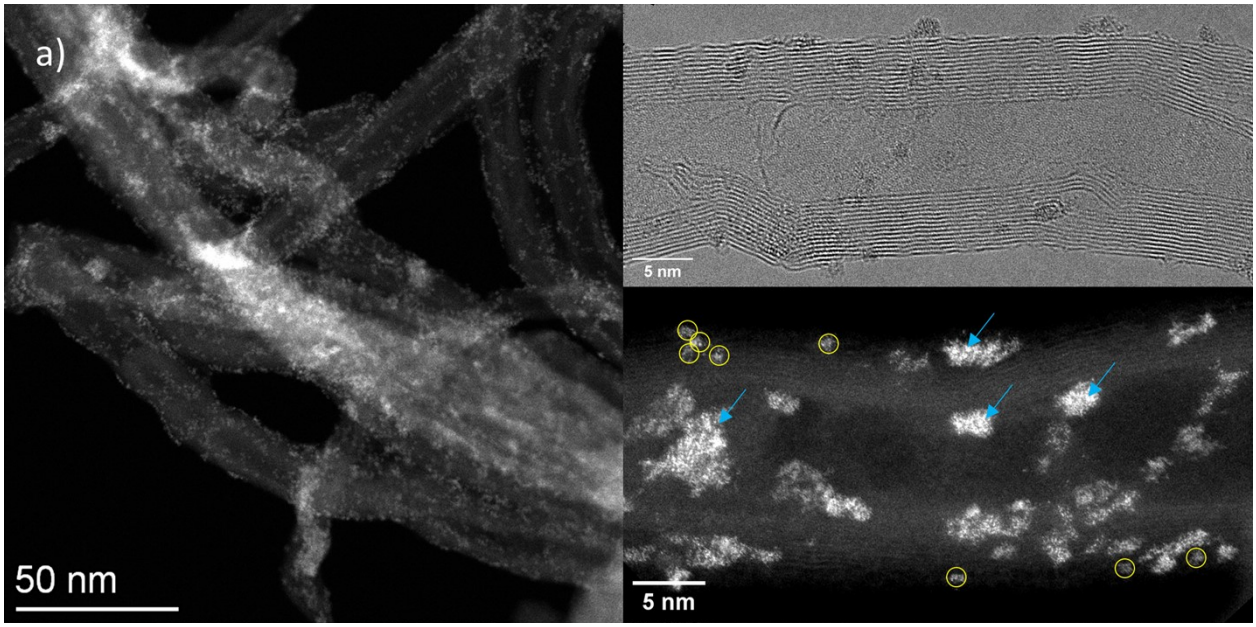

Figure S7. HAADF-STEM and HRTEM images of 14% $PW_{11}Zr$/Zn-CNT. In the high-resolution HAADF-STEM images, yellow circles indicate individual Zr-POM particles, blue arrows indicate agglomerates of Zr-POM particles formed under the action of the electron beam.

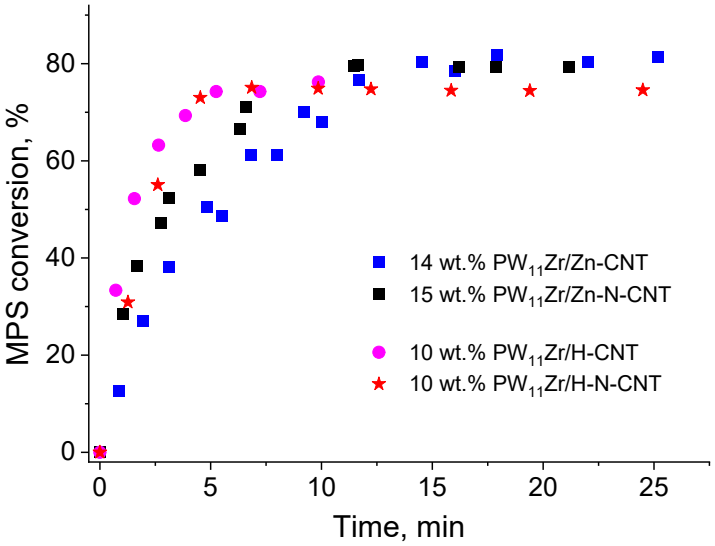

Figure S8. Effects of the support and immobilizing agent nature on the rate of MPS oxidation with 30% H_2O_2 over immobilized $PW_{11}Zr$ catalysts. Reaction conditions: [MPS] = 0.1 M, [H_2O_2] = 0.1 M, 0.1 μmol Zr-POM, 1 ml CH_3CN, 27 °C.

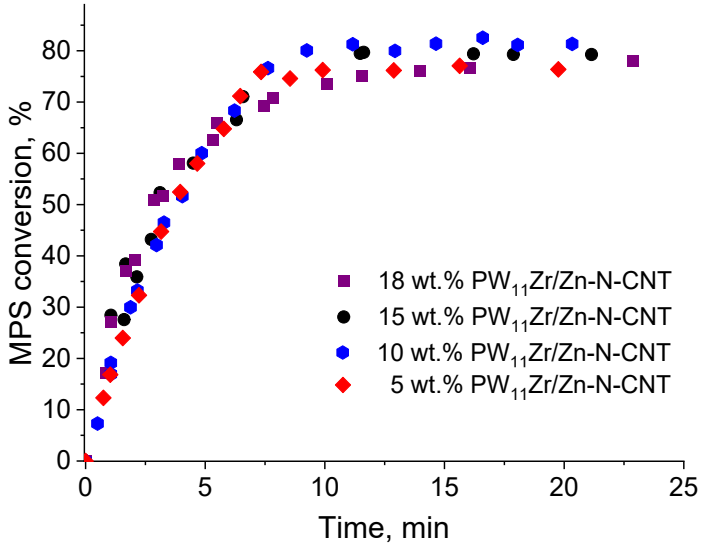

Figure S9. Kinetic curves for MPS oxidation with 30% H_2O_2 over $PW_{11}Zr$/Zn-N-CNT catalysts with varied $PW_{11}Zr$ content. Reaction conditions: [MPS] = 0.1 M, [H_2O_2] = 0.1 M, 0.1 μmol Zr-POM, 1 ml CH_3CN, 27 °C.

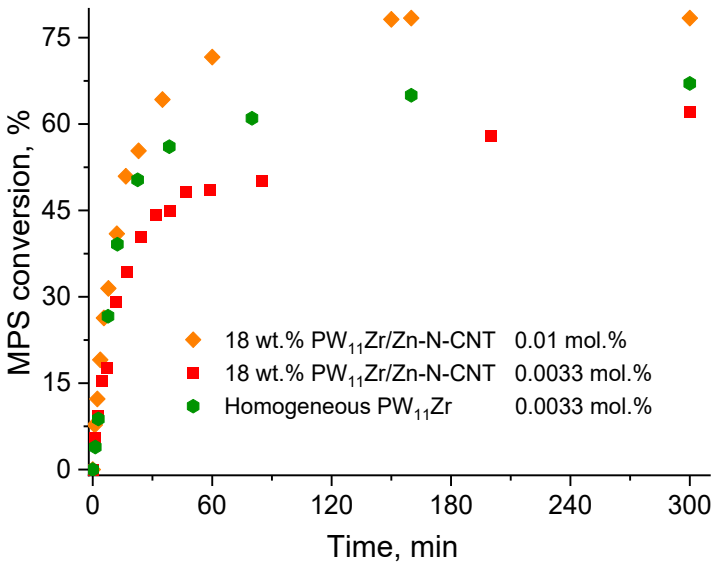

Figure S10. Kinetic curves of MPS oxidation with 30% H_2O_2 in the presence of 18 wt.% $PW_{11}Zr$/Zn-N-CNT and homogeneous $PW_{11}Zr$. Reaction conditions: [MPS] = 0.1 M, [H_2O_2] = 0.1 M, 0.0033 or 0.0094 mol.% Zr-POM, 10 ml CH_3CN, 27 °C.

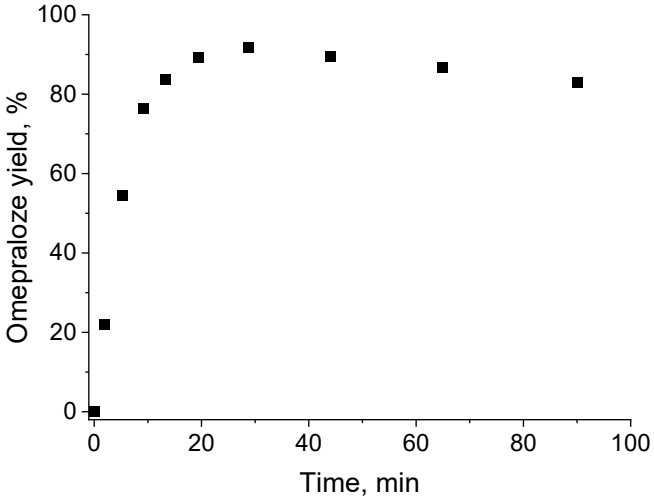

Figure S11. Kinetic curve for omeprazole sulfide oxidation with 30% aqueous H_2O_2 over 18% $PW_{11}Zr$/N-CNT catalyst. Reaction conditions: [omeprazole sulfide] = 0.05 M, [H_2O_2] = 0.05 M, 0.1 μmol Zr-POM, 1 ml CH_3CN, 27 °C.

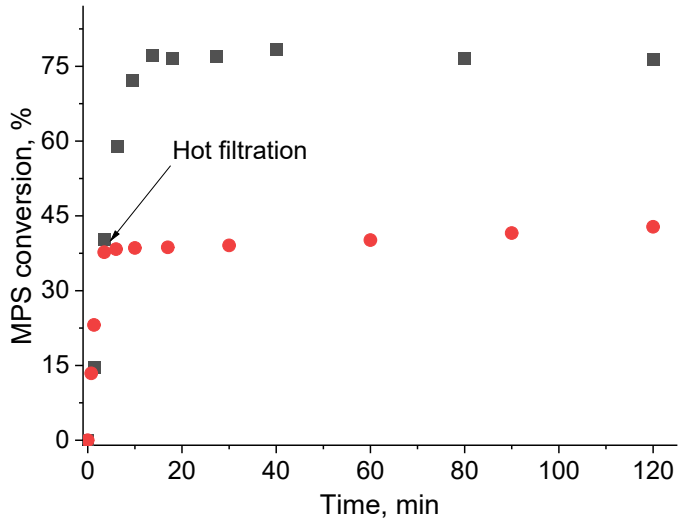

Figure S12. Hot filtration test for MPS oxidation with 30% aq. H_2O_2 over 18 wt.% $PW_{11}Zr$/Zn-N-CNT in ethanol. Reaction conditions: [MPS] = 0.1 M, [H_2O_2] = 0.1 M, 0.05 μmol Zr-POM, 1 ml ethanol, 60 °C.

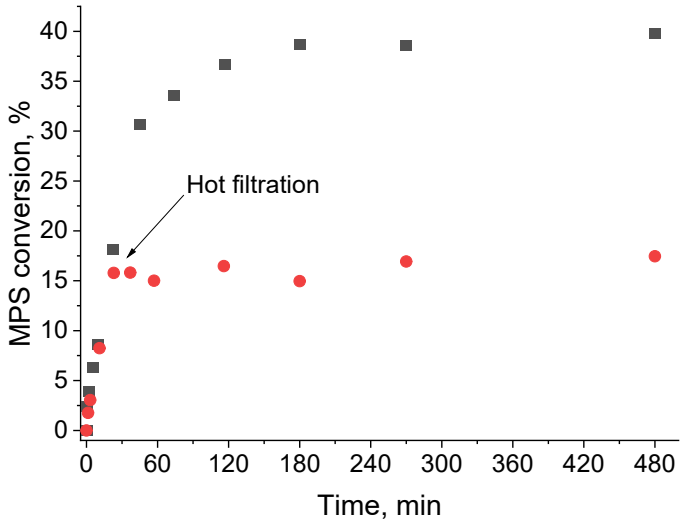

Figure S13. Hot filtration test for MPS oxidation with 30% aq. H_2O_2 over 10 wt.% $P_2W_{17}Zr$/Zn-N-CNT in ethanol. Reaction conditions: [MPS] = 0.1 M, [H_2O_2] = 0.1 M, 0.1 μmol Zr-POM, 1 ml ethanol, 27 °C.

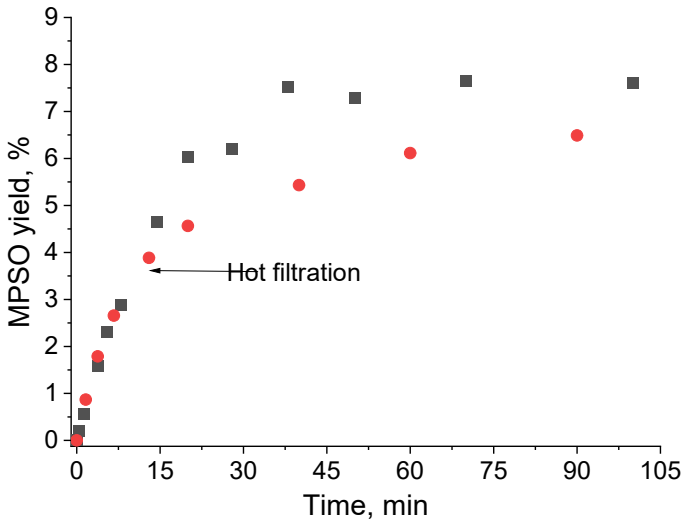

Figure S14. Hot filtration test for MPS oxidation with 30% aq. H_2O_2 over 10 wt.% $PW_{11}Ti$/Zn-N-CNT in ethanol. Reaction conditions: [MPS] = 0.1 M, [H_2O_2] = 0.1 M, 0.1 μmol Ti-POM, 1 ml ethanol, 60 °C.

Table S1. Comparison of Zr-POM content in Zr-POM/(N)-CNT based on TGA and UV-vis.

Catalyst	Amount of Zr-POM based on UV-vis, wt.%	Amount of Zr-POM based on TGA, wt.%
ZrW_5/Zn-N-CNT	13	16
ZrW_5/Zn-CNT	13	14
ZrW_5/H-N-CNT	11	11
$P_2W_{17}Zr$/Zn-N-CNT	19	22
$P_2W_{17}Zr$/Zn-CNT	12	12
$P_2W_{17}Zr$/H-N-CNT	23	24
$PW_{11}Zr$/Zn-CNT	13	14
$PW_{11}Zr$/Zn-N-CNT	18	20
$PW_{11}Zr$/H-N-CNT	16	16

Table S2. Textural data for CNT and N-CNT supports and representative supported Zr-POM catalysts.

Catalyst / Support	S_{BET}, m^2/g	V_{pore}, cm^3/g
CNT	148	0.70
14 wt.% $PW_{11}Zr$/Zn-CNT	119	0.63
1.8 at.% N-doped CNT	157	0.61
10 wt.% ZrW_5/Zn-N-CNT	120	0.54
15 wt.% ZrW_5/Zn-N-CNT	112	0.50
18 wt.% $PW_{11}Zr$ /Zn-N-CNT	110	0.47

Table S3. Elemental composition of TBA-salt $PW_{11}Zr$, N-CNT support and $PW_{11}Zr$/Zn-N-CNT catalyst based on XPS data.

	C		O		N		Cl		Zr		W		P		Zn	
	at.	wt.	at.	wt.	at.	wt.	at.	wt.	at.	wt.	at.	wt.	at.	wt.	at.	wt.
TBA-salt $PW_{11}Zr$	57.9	32.5	34.4	25.7	2.3	1.5	-	-	0.6	2.6	4.3	37.0	0.5	0.7	-	-
N-CNT	95.5	94.2	2.9	3.8	1.5	1.7	0.1	0.3	-	-	-	-	-	-	-	-
15% $PW_{11}Zr$/Zn-N-CNT	87.9	74.0	9.05	10.2	1.5	1.5	0.05	0.1	0.1	0.6	0.9	11.6	0.1	0.2	0.4	1.8

Table S4. Blank experiments and effect of $Zn(NO_3)_2$ additives on catalytic performance.

№	Catalyst + additive	Loading, mM/mg	Time, min	MPS conv., %	MPSO select., %	$MPSO_2$ select., %
1	$PW_{11}Zr$	1/7.5	<1	80	91	9
2	$PW_{11}Zr$ + $Zn(NO_3)_2$, 6 equiv. to POM	1+6/ 7.5+1.8	1	75	85	15
3	$PW_{11}Zr$	0.1/0.75	3	74	85	13
4	18% $PW_{11}Zr$/Zn-N-CNT	0.1/4.2	10	80	88	11
5	N-CNT	-/5	180	1	0	0
6	N-CNT + $Zn(NO_3)_2$, 10 equiv. to N	-/5+22	180	40	95	4
7	CNT	-/5	180	5	95	4
8	CNT + of $Zn(NO_3)_2$, same amount as for N-CNT	-/5+22	180	7	96	3

Reaction conditions: [MPS] = 0.1 M, [H_2O_2] = 0.1 M, 1 ml CH_3CN, 27 °C.

Table S5. Comparison of catalytic performance of various heterogeneous catalysts for selective oxidation of MPS with 30% H_2O_2.

Catalyst	[MPS], M	[H_2O_2], M	Catalyst, mol. %[a]	T, °C	Solvent	Time, min	MPS conv., %	Selectivity, %		H_2O_2 eff., %	TON [b]	TOF, h^{-1} [c]	Heterogen. nature of catalysis[d]	Ref.
								MPSO	$MPSO_2$					
$PW_{11}Zr$/Zn-N-CNT	0.1	0.1	0.1	27	CH_3CN	10	80	88	12	90	880	10200	+	This work
$PW_{11}Zr$/Zn-N-CNT	0.1	0.1	0.01	27	CH_3CN	130	78	87	12	84	9360	n.d.	+	This work
UiO-66	0.1	0.1	4	25	CH_3CN	15	48	1	99	96	24	180	+	[S9]
Zr-MMM-E	0.1	0.1	1.3	60	CH_3CN	60	57	37	63	93	71	130	+	[S10]
PW_4/CNT	0.1	0.1	1	27	CH_3CN	150	93	90	10	99	99	106	+	[S11]
PW_4-PIILP	0.33	0.83	0.5	45	CH_3OH	15	95	96	4	n.d.	200	760	+	[S12]
PW_4-Zn/SnO_2	0.1	0.1[h]	0.7	20	DMC	7	87	84	16	99	143	n.d.	+	[S13]
WO_3-Zn/SnO_2	0.1	0.1[h]	0.5	20	DMC	90	84	81	19	99	200	n.d.	+	[S14]
W-MMM-E	0.1	0.1	1	25	CH_3CN	300	91	91	9	99	106	120	+	[S15]
$[W_{10}O_{32}]^{4-}$/SiO_2-NH_3^+	0.2	0.23	0.1	25	CH_3OH/ CH_2Cl_2	90	97	95	5	98	960	n.d.	+	[S16]
[VO_2(sal-ambmz)]-Y	0.25	0.25	0.036	25	CH_3CN	120	96	97	3	98	2750	1345	+	[S17]
$[C_4mim]_3[PMo_{12}O_{40}]$	0.1	0.11	2	25	CH_3OH	30	99	98	2	91	50	n.d.	n.d.	[S18]
$[MoO_2(O_2)(L)_2]^{2-}$-MRA	1	2	0.1	25	CH_3OH	40	>99	>99	<1	n.d.	980	1470	+	[S19]
Polymerized ionic network (PIN) viologen	0.25	0.5	7.8[e]	60	CH_3OH	70	99	97	3	n.d.	13	n.d.	+	[S20]
TS-1-Lam	0.4	0.2	0.45	25	CH_3CN	120	50	99	1	n.d.	118	324	n.d.	[S21]
TS-1	8.3[f]	11.6	0.2	25	no solv.	120	65	81	12	n.d.	230	n.d.	+	[S22]
Ti-IEZ-MMW	8.3[f]	11.6	0.2	25	no solv.	120	99	94	6	99	490	n.d.	+	[S21]
Ti-MMM-2	0.1	0.12	1.6	20	CH_3CN	35	98	76	24	n.d.	74	100	+	[S23]
Ti-Beta	0.1	0.3	2	40	CH_3CN	30	93	65	35	n.d.	62	n.d.	n.d.	[S24]
Ti-MCM-41	0.1	0.3	1.3	40	CH_3CN	30	80	75	25	n.d.	77	n.d.	n.d.	[S23]
Ti-FER-12.5 Dark	0.02[f]	0.1	5	25	CH_3CN	250	80	95	5	>95	17	14	n.d.	[S25]

[a] Catalyst mol.% was determined as the ratio of moles of substrate per moles of active sites under the assumption that all metal (active compound) sites are accessible for reactants; [b]TON (turnover number) = (moles of MPSO + 2 × moles $MPSO_2$ generated) / moles of catalyst; [c]TOF (turnover frequency) = moles of substrate consumed / (moles of catalyst × time), determined from initial rates of substrate consumption or taken from reported data; n.d. – not determined (no kinetic data were provided); [d] "+" – proved by hot filtration test, n.d. – the nature of catalysis was not determined; [e]calculated under the assumption that each viologen residue is a catalytically active site; [f]1 mmol of neat MPS was used and 1.2 mmol of 35% H_2O_2, [MPS] = 8.3 M and [H_2O_2] = 11.6 M; [g]Diphenyl sulfide was used as a substrate, [h]60% H_2O_2 was used.

References

[S1] R. Villanneau, H. Carabineiro, X. Carrier, R. Thouvenot, P. Herson, F. Lemos, F. Ramoa Ribeiro, M. Che, Synthesis and characterization of Zr (IV) polyoxotungstates as molecular analogues of zirconia-supported tungsten catalysts, *J. Phys. Chem. B*, 2004, **108**, 12465−12471.

[S2] K. Nomiya, Y. Saku, S. Yamada, W. Takahashi, H. Sekiya, A. Shinohara, M. Ishimaru, Y. Sakai, Synthesis and Structure of Dinuclear Hafnium(IV) and Zirconium(IV) Complexes Sandwiched between 2 Mono-Lacunary α-Keggin Polyoxometalates, *Dalton Trans*., 2009, 5504.

[S3] N. V. Maksimchuk, S. M. Marikovskaya, K. P. Larionov, A. A. Antonov, M. V. Shashkov, V. V. Yanshole, V. Yu. Evtushok, O. A. Kholdeeva, Tuning Reactivity of Zr-Substituted Keggin Phosphotungstate in Alkene Epoxidation through Balancing H_2O_2 Activation Pathways: Unusual Effect of Base, *Inorg. Chem.*, 2023, **62**, 18955−18969.

[S4] O. A. Kholdeeva, G. M. Maksimov, R. I. Maksimovskaya, M. P. Vanina, T. A. Trubitsina, D. Yu. Naumov, B. A. Kolesov, N. S. Antonova, J. J. Carbó, J. M. Poblet, Zr(IV)-Monosubstituted Keggin-Type Dimeric Polyoxometalates: Synthesis, Characterization, Catalysis of H_2O_2-based Oxidations, and Theoretical Study, *Inorg. Chem.*, 2006, **45**, 7224−7234.

[S5] Y. Saku, Y. Sakai, K. Nomiya, Relation Among the 2:2-, 1:1- and 1:2-type Complexes of Hafnium(IV)/Zirconium(IV) with Mono-Lacunary α_2-Dawson Polyoxometalate Ligands: Synthesis and Structure of the 2:2-Type Complexes $[\{\alpha_2\text{-}P_2W_{17}O_{61}M(\mu\text{-}OH)(H_2O)\}_2]^{14-}$ (M=Hf, Zr), *Inorg. Chim. Acta* 2010, **363**, 967−974.

[S6] W. G. Klemperer, *Introduction to Early Transition Metal Polyoxoanions* in *Inorg. Synth.*, A. P. Ginsberg (Ed.), 1990; Vol. 27, pp 71−132.

[S7] O.A. Kholdeeva, G.M. Maksimov, R.I. Maksimovskaya, L.A. Kovaleva, M.A. Fedotov, V.A. Grigoriev, C.L. Hill, A Dimeric Titanium-Containing Polyoxometalate. Synthesis, Characterization, and Catalysis of H_2O_2-Based Thioether Oxidation, *Inorg. Chem.*, 2000, **39**, 3828−3837.

[S8] R.J. Errington, B. Kandasamy, D. Lebbie, T. Izuagie, in *Polyoxometalate-Based Assemblies and*

Functional Materials. Structure and Bonding; (Ed.: Y.F. Song); Springer: Cham, 2017, Vol. 176, pp 139−163.

[S9] V. Y. Evtushok, K. P. Larionov, V. A. Lopatkin, O. A. Stonkus, O. A. Kholdeeva, What factors determine activity of UiO-66 in H_2O_2-based oxidation of thioethers? The role of basic sites, *J. Catal.*, 2023, **427**, 115099.

[S10] I. D. Ivanchikova, O. V. Zalomaeva, N. V. Maksimchuk, O. A. Stonkus, T. S. Glazneva, Y. A. Chesalov, A. N. Shmakov, M. Guidotti, O. A. Kholdeeva, Alkene Epoxidation and Thioether Oxidation with Hydrogen Peroxide Catalyzed by Mesoporous Zirconium-Silicates, *Catalysts*, 2022, **12**, 742.

[S11] V. Y. Evtushok, I. D. Ivanchikova, O. Y. Podyacheva, O. A. Stonkus, A. N. Suboch, A. Y. Chesalov, O. V. Zalomaeva, O. A. Kholdeeva, Carbon nanotubes modified by Venturello complex as highly efficient catalysts for alkene and thioethers oxidation with hydrogen peroxide, *Front. Chem.*, 2019, **7**, 858.

[S12] S. Doherty, J. G. Knight, M. A. Carroll, J. R. Ellison, S. J. Hobson, S. Stevens, C. Hardacre and P. Goodrich, Efficient and selective hydrogen peroxide-mediated oxidation of sulfides in batch and segmented and continuous flow using a peroxometalate-based polymer immobilised ionic liquid phase catalyst, *Green Chem.*, 2015, **17**, 1559-1571.

[S13] S. Nojima, K. Kamata, K. Suzuki, K. Yamaguchi, N. Mizuno, Selective Oxidation with Aqueous Hydrogen Peroxide by $[PO_4\{WO(O_2)_2\}_4]^{3-}$ Supported on Zinc-Modified Tin Dioxide, *ChemCatChem*, 2015, **7**, 1097-1104.

[S14] K. Kamata, K. Yonehara, Y. Sumida, K. Hirata, S. Nojima, N. Mizuno. Efficient heterogeneous epoxidation of alkenes by a supported tungsten oxide catalyst, *Angew. Chem. Int. Ed.*, 2011, **50**, 12062-12066.

[S15] N. Maksimchuk, I. Ivanchikova, O. Zalomaeva, Y. Chesalov, A. Shmakov, V. Zaikovskii, O. Kholdeeva, Tungsten-based mesoporous silicates W-MMM-E as heterogeneous catalysts for liquid-phase oxidations with aqueous H_2O_2, *Catalysts*, 2018, **8**, 95.

[S16] F. Bigi, A. Corradini, C. Quarantelli, G. Sartori, Silica-bound decatungstates as heterogeneous catalysts for H_2O_2 activation in selective sulfide oxidation, *J. Catal.*, 2007, **250**, 222-230.

[S17] M. R. Maurya, A. K. Chandrakar, S. Chand, Oxidation of phenol, styrene and methyl phenyl sulfide with H_2O_2 catalysed by dioxovanadium(V) and copper(II) complexes of 2-aminomethylbenzimidazole-based ligand encapsulated in zeolite-Y, *J. Mol. Catal. A: Chem.*, 2007, **263**, 227-237.

[S18] P. Zhao, M. Zhang, Y. Wu, J. Wang, Heterogeneous Selective Oxidation of Sulfides with H_2O_2 Catalyzed by Ionic Liquid-Based Polyoxometalate Salts, *Ind. Eng. Chem. Res.*, 2012, **51**, 6641-6647.

[S19] J. J. Boruah, S. P. Das, S. R. Ankireddy, S. R. Gogoi, N. S. Islam, Merrifield resin supported peroxomolybdenum(vi) compounds: recoverable heterogeneous catalysts for the efficient, selective and mild oxidation of organic sulfides with H_2O_2, *Green Chem.*, 2013, **15**, 2944-2959.

[S20] S. Hou, N. Chen, P. Zhang, S. Dai, Heterogeneous viologen catalysts for metal-free and selective oxidations, *Green Chem.*, 2019, **21**, 1455-1460.

[S21] I. Martausová, D. Spustová, D. Cvejn, A. Martaus, Z. Lacný, J. Přech, Catalytic activity of advanced titanosilicate zeolites in hydrogen peroxide S-oxidation of methyl(phenyl)sulfide, *Catal. Today*, 2019, **324**, 144-153.

[S22] Y. Kon, T. Yokoi, M Yoshioka, S. Tanaka, Y. Uesaka, T. Mochizuki, K. Sato, T. Tatsumi, Selective hydrogen peroxide oxidation of sulfides to sulfoxides or sulfones with MWW-type titanosilicate zeolite catalyst under organic solvent-free conditions, *Tetrahedron*, 2014, **70**, 7584-7592.

[S23] O. A. Kholdeeva, M. S. Mel'gunov, A. N. Shmakov, N. N. Trukhan, V. V. Kriventsov, V. I. Zaikovskii, M. E. Malyshev, V. N. Romannikov, A new mesoporous titanium-silicate Ti-MMM-2: a highly active and hydrothermally stable catalyst for H_2O_2-based selective oxidations, *Catal. Today*, 2004, **91**, 205-209.

[S24] A. Corma, M. Iglesias, F. Sanchez, Large pore Ti-zeolites and mesoporous Ti-silicalites as catalysts for selective oxidation of organic sulfides, *Catal. Lett.*, 1996, **39**, 153-156.

[S25] M. Radko, M. Rutkowska, A. Kowalczyk, P. Mikrut, A. Święs, U. Díaz, A. E. Palomares, W. Macyk, L. Chmielarz, Catalytic oxidation of organic sulfides by H_2O_2 in the presence of titanosilicate zeolites, *Micropor. Mesopor. Mater.*, 2020, **302**, 110219.